(Preprint) AAS 18-211

NUMERICAL CHALLENGES IN CASSINI MANEUVER OPERATIONS

Mar Vaquero* **and Yungsun Hahn**

Launched in 1997 to observe Saturn and its system, Cassini successfully entered Saturn orbit in 2004 and impacted the planet on September 15, 2017 after 22 orbits each skimming over Saturn's cloud tops. The Cassini mission represents the most complex gravity-assist trajectory ever flown. As such, the Flight Path Control team encountered many difficulties along the way, resulting in a continuously evolving maneuver process. In this paper, we focus on the challenges presented by the well-known singularities in the transfer problem and the unexpected numerical instabilities in state propagations through flybys, maneuver algorithm convergence issues, and orbital element targeting difficulties.

OVERVIEW

Launched on October 15, 1997 to observe Saturn and its moons, rings, and magnetosphere, the Cassini-Huygens spacecraft successfully entered Saturn orbit on July 1, 2004 and impacted the planet on September 15, 2017. The last phase of the mission, called the Grand Finale (GF), was a series of 22 highly inclined (62 degrees), short period (6.5 days), ballistic orbits each passing within a few thousand kilometers of the cloud tops of Saturn.[1] On September 15, 2017, the spacecraft dove into Saturn's atmosphere and became permanently captured. The end of mission trajectory depicted in Figure 1 was incorporated in the final phase of the Solstice Mission after multiple studies were carried out to ensure that, per Planetary Protection requirements and before the spacecraft ran out of propellant, the possibility of future impact with any of the large icy moons, such as Enceladus, was precluded.

The Cassini mission arguably represents the most complex gravity-assist trajectory ever flown,[2–4] and the last few orbits – although no moon flybys were targeted – were no less. As such, the Cassini Flight Path Control team encountered many difficulties along the way. Flying the spacecraft on such a complex trajectory was a challenging task and the maneuver processes evolved and improved on a daily basis. The nominal navigation strategy consisted of scheduling three Orbit Trim Maneuvers (OTM) between each targeted encounter, as illustrated in Figure 2 for an outbound-to-inbound leg. Note that an outbound flyby occurs after pericrone (Saturn periapsis) whereas an inbound encounter occurs before pericrone. A cleanup maneuver, about three days after an encounter, removes the orbital dispersion errors incurred by inaccuracies in the flyby conditions; a shaping maneuver, normally located near apoapsis, targets the encounter conditions; and an approach maneuver, about three days before an encounter, refines the orbit before an encounter, if necessary.

Throughout the design cycles of 493 maneuvers, a variety of challenges – from the well-known singularities in the transfer problem to numerical instabilities in state propagations through flybys

*NASA Jet Propulsion Laboratory, California Institute of Technology

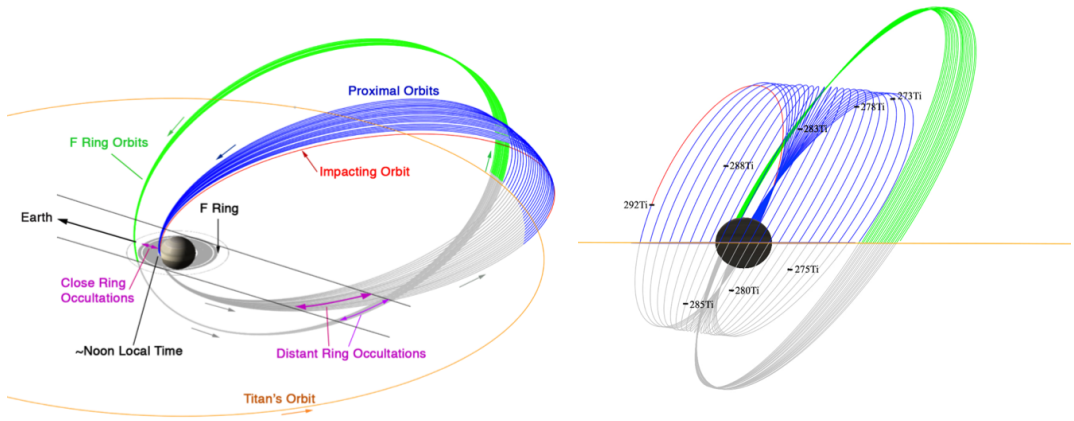

(a) (b)

Figure 1. Representation of Cassini's Grand Finale trajectory encompassing the F-ring orbits (green), the Grand Finale orbits (blue), and the final orbit (red) culminating with Saturn atmospheric entry on September 15, 2017.

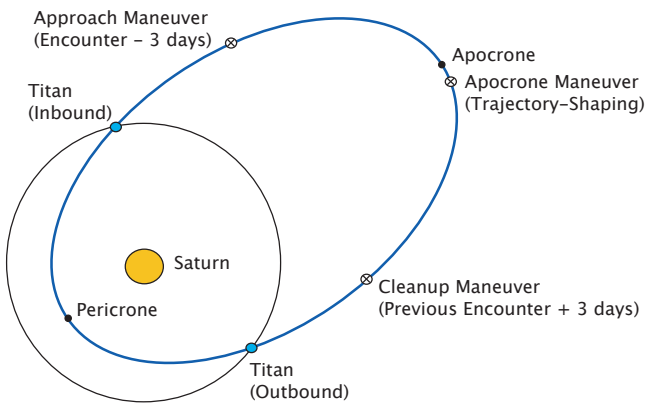

Figure 2. Navigation Strategy of Three Maneuvers per Flyby for Saturn Tour

and orbital element targeting difficulties – were faced and overcome. These numerical challenges experienced during flight are grouped and discussed by maneuver type, i.e., a) flyby cleanup maneuvers, b) shaping/targeting maneuvers, and c) flyby approach maneuvers.

CHALLENGES FACED DURING CLEANUP MANEUVER DESIGNS

The numerical difficulties encountered during cleanup maneuvers applied especially to Titan flybys and resulted in large ΔV magnitude discrepancies between pre-flyby and post-flyby solutions. Additionally, certain Titan flybys caused instability in the right ascension and declination values of the designed maneuver using post-flyby orbit determination data. This difference in post-flyby solutions caused problems for the Attitude Control team, who produced solutions with very different wheel speed profiles. In such scenarios, the Flight Path Control team chose to fix the burn direction to alleviate the problem. Two representative examples of such challenging designs are OTM257 and OTM338, discussed below.

OTM257 Targeting to Titan-71

Orbit Trim Maneuver 257 was the cleanup maneuver after the Titan-71 flyby, targeting the inbound Enceladus-11 flyby on August 13, 2010. The main engine burn began at 1:14 AM PDT and telemetry immediately after the maneuver showed a burn duration of 4.829 seconds, giving a ΔV of 0.825 m/s (see Table 1 for additional burn statistics). Throughout the maneuver design cycle, the wheel speed profile for OTM257 was stable and consistent. However, even though the flyby was within 1-sigma of the pre-flyby solution, OTM257 went from an RCS size pre-flyby to an ME size with a high cancellation penalty – more than 8 m/s – due to the large asymptote change, as illustrated by the cancellation cost contour in Figure 3. This contour plot is a two-dimensional linear representation of a larger six-dimensional solution; by using contours plotted with $B \cdot R$ and $B \cdot T$ components, it is possible to view the effects on ΔV for various encounter positions in the B-plane.[5] This type of plot was regularly used in operations mainly to help determine if an approach maneuver and/or a cleanup maneuver could be canceled, but and also as a linear check of an integrated solution.

The cancellation plot from OTM257 shows a small but thin pre-flyby OD ellipse (cyan) and the post-flyby ellipse appears as a point (red). Because of the angle between the pre-flyby ellipse and the contour lines, the increase in the flyby error from roughly 0.5 km to 2 km drastically increased the ΔV penalty, quadrupling the magnitude of the cleanup maneuver from 0.21 m/s to 0.84 m/s.

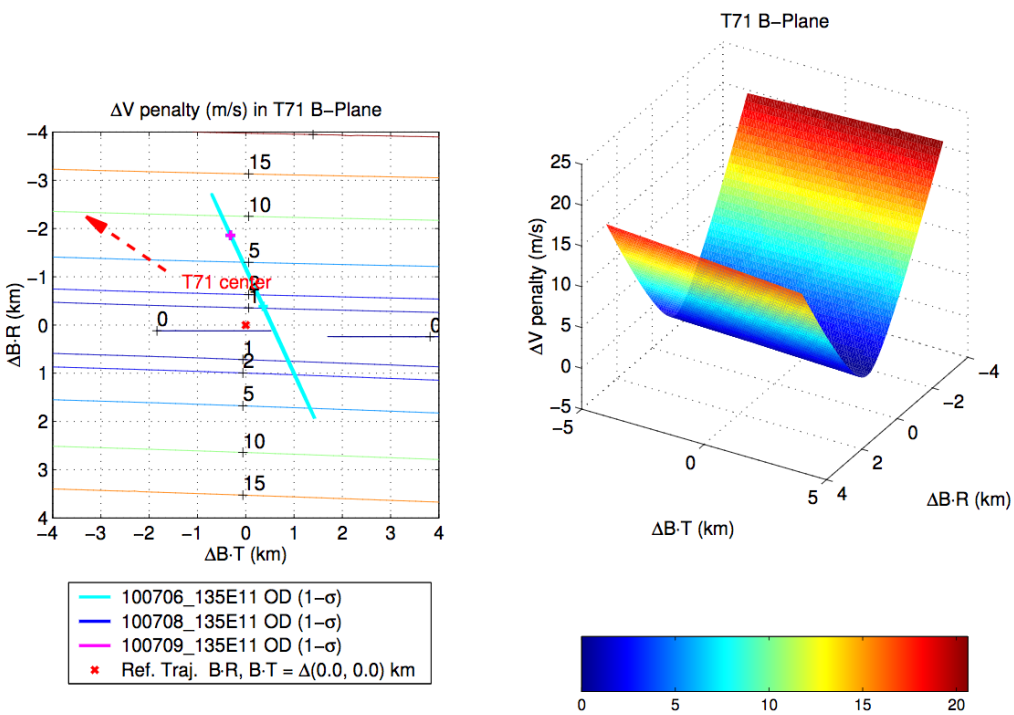

Figure 3. Post Titan-71 OTM257 Cancellation Cost Contour

In addition to the increase in ΔV, the cancelation of OTM257 also caused large deviations from the reference trajectory in subsequent transfers. Figures 4(a)-4(b) illustrate the position deviations from Titan-71 to Enceladus-11 and from Enceladus-11 to Titan-72, respectively, showing in both cases a downstream pericrone change of more than 16,000 km.

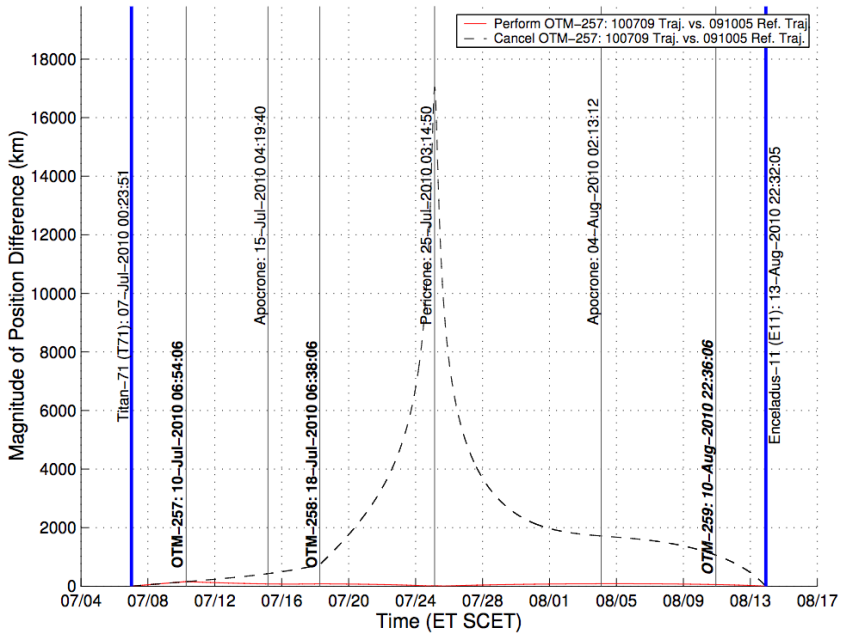

T71 to E11 = 37.9 days, 1.5 revs., 3 mvrs. (2 deterministic, 1 statistical)

(a) Trajectory Deviations from Titan-71 to Enceladus-11

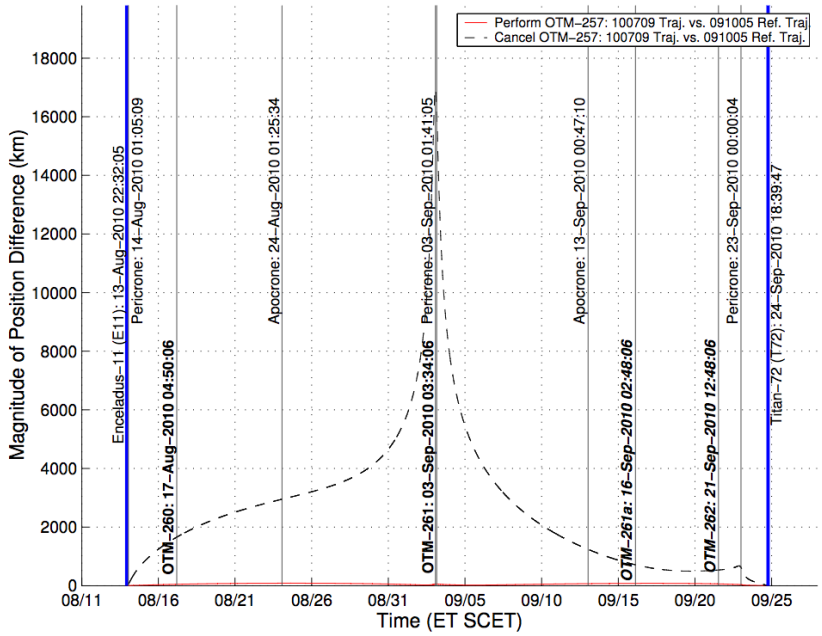

E11 to T72 = 41.8 days, 2.5 revs., 4 mvrs. (2 deterministic, 2 statistical)

(b) Trajectory Deviations from Enceladus-11 to Titan-72

Figure 4. Norm of the inverse of the K-matrix as a function of time: minimum point on the curve represents the optimal location for maneuver placement between periapsis-6 and periapsis-7 with the target fixed at periapsis-12.

OTM338 Targeting to Titan-88

OTM338 is a representative example of a case in which the Flight Path Control Team decided to constrain the ΔV direction to reduce sensitivities in the chain optimization process and avoid having drastic variations in the wheel speed profile due to changes in the right ascension and declination of the maneuver design. The pre-flyby design for OTM338 showed a burn magnitude of roughly 0.3 m/s, which is main engine size, and an ME burn is performed with the wheels stopped after the yaw turn. Consequently, wheel speed issues during the subsequent roll turn are rare. The post-flyby design became quite different, with the size of OTM338 being less than a tenth of the pre-fly design. While the wheel speed profile was acceptable for the preliminary (pre-flyby) solution, there were intermediate OD solutions which resulted in roll/yaw turn angle changes of more than 30 degrees, causing wheel speeds problems for the Attitude Control team. Because OTM338 was small compared to OTM339 (0.028 m/s vs 1.66 m/s), the optimal solution for OTM338 was sensitive to slight changes to the orbit determination solution. This numerical sensitivity was caused by the presence of multiple solutions that added up to nearly the same total. This 'wobbling' was worse for RCS size designs, but it also occurred for smaller ME size designs. For the first post Titan-88 maneuver design, the wheel speeds were found acceptable. With more post-flyby tracking data, the direction of OTM338 substantially changed, rendering the prior wheel speed strategy inadequate. Hence, instead of rushing to find a new wheel speed solution for OTM338, the maneuver direction could have been constrained to the prior ΔV direction which yielded favorable wheel speeds. The key assumption here is that a near optimal solution in the direction of the first post-flyby design should exist. Although the final maneuver design did not need to be constrained in the direction of the first post-flyby maneuver solution, it was in a similar direction. As a result of this experience, it was decided that future optimized cleanup maneuvers sensitive to the OD solution would be constrained to the direction of the first post-flyby maneuver's direction (see Table 1 for additional burn statistics).

Table 1. Burn Statistics for Selected Cleanup Maneuvers

	OTM257	OTM338
Orbit Location	Titan-71 + 3 days	Titan-88 + 4 days
Maneuver Time	10-JUL-2010 06:53:00	02-DEC-2012 23:32:00
Targeting Body	Enceladus	Titan
Days to Encounter	34.7 days	76.1 days
Distance to Saturn	36.2 Saturn Radii	28.3 Saturn Radii
Flyby Altitude	2551.6 km	1978.1 km
True Anomaly	164.82 deg	175.81 deg
ΔV Magnitude	0.8320 m/s	0.0276 m/s
Right Ascension	296.89 deg	227.95 deg
Declination	-16.34 deg	-47.66 deg
Roll Turn	85.36 deg	153.23 deg
Yaw Turn	-60.93 deg	-142.38 deg
Burn Time	5.03 sec	21.80 sec
Burn Type	Main Engine	Reaction Control System

CHALLENGES DURING TARGETING MANEUVER DESIGNS

Orbital dynamics issues were encountered notably during targeting maneuvers placed at or near apoapsis, resulting in no viable either prime or backup options. In particular, there are two cases of interest discussed in this section; OTM159, which was the shape-changing maneuver that provided transition from the prime mission to the extended mission and OTM300, the targeting maneuver to a double flyby, Dione-3 and Titan-79. There were also instances of pure numerical issues during the design of targeting maneuvers, where a very small difference in the propagator tolerance led to a significant difference in the B-Plane aimpoint parameters. Such situation was encountered during the design of OTM450, the targeting maneuver to one of the last Titan flybys in the mission.

Orbital Dynamics Instabilities

OTM159 – Transitioning from the Prime Mission to the Extended Mission OTM159 was the periapsis maneuver setting up the Titan-45 encounter on July 29, 2008 The Main Engine burn began at 12:45 a.m. PDT and telemetry immediately after the maneuver showed the burn duration was 73.5 seconds, resulting in a ΔV of 12.2 m/s (see additional maneuver statistics in Table 2). However, the backup location for OTM159 incurred much more ΔV (32 m/s) than its nominal location (12 m/s). Of even larger concern, the downstream cost of using the backup location was almost 97 m/s – a prohibitively large penalty for delaying a shaping maneuver. In an effort to reduce this cost, several options that involved altering downstream encounters to absorb the ΔV at the expense of deviating from the reference trajectory were investigated. In fact, the most promising strategy consisted of moving the backup location by a week, thus reducing the ΔV cost from 32 m/s to 19 m/s by eliminating an Enceladus flyby (E6) and altering seven Titan flybys downstream (from Titan-45 to Titan-51). In such scenario, the cost of using the backup location would have been decreased to 8 m/s in exchange of missing valuable science observations. To reduce the likelihood of invoking such unfavorable measures, the decision was made to uplink the files early to provide additional uplink windows should the need arise. In the end, OTM159 was executed nominally on June 23, 2008 and there was no need to resort to the backup strategy.

OTM300 – Targeting a Double Moon Flyby This targeting burn was the periapsis maneuver setting up for the Titan-79 encounter on December 13, 2011. The main engine burn began at 10:45 PM PST and telemetry immediately after the maneuver showed a burn duration of 17.175 seconds, giving a ΔV of 2.969 m/s (see additional maneuver statistics in Table 2). While the maneuver targeted to Titan-79, the next encounter was actually a 100 km flyby of Dione (D-3), taking place one day before the Titan-79 encounter. Therefore, OTM300 set up the trajectory for the dual Dione/Titan flybys. Additional effort was required to ensure that Titan-79 was targeted rather than D-3, since not both could be independently targeted, and to make sure the resulting untargeted flyby was still safe and the spacecraft was off an impactor. The main reason for ensuring that the Titan flyby was accurately was to prevent having a ΔV penalty downstream resulting from a Titan flyby miss of tens of kilometers. Titan had, by far, the most effect on the reference trajectory and subsequent flybys. Because OTM300 had a relatively large deterministic ΔV cost (3 m/s) and was executed only 45 minutes from periapsis, delaying to the backup maneuver location turned to be very costly in terms of propellant consumption (7.2 m/s). Due to this sensitivity, the maneuver was designed early enough to enable six uplink opportunities, thereby eliminating the possibility of a delay to the backup time due to Deep Space Network (DSN) transmitter failure. Nonetheless, other failures were possible, so at least one viable backup scenario had to be identified. The Navigation Team came up with two potential backup scenarios:

- C1 represented the backup strategy "as is", without modification to the flyby targets. When compared to the OTM300 prime case (i.e., everything goes as planned, and no backup maneuver is necessary), C1 exhibited a downstream cost of 9.8 m/s.

- C2 aimed for an altered target at Titan-79, while maintaining the reference targets of all encounters downstream. In other words, following this strategy, the target accuracy at Titan-79 would have not been met, but the following encounter targets would have been preserved. When compared to the nominal strategy, i.e., no backup maneuver necessary, C2 exhibited a downstream cost of about 8.7 m/s.

After all, there was no need to resort to the backup maneuver in this case either since OTM300 was executed nominally on November 23, 2011.

Table 2. Burn Statistics for Selected Targeting Maneuvers

	OTM159	OTM300	OTM450
Orbit Location	Titan-44 periapsis	Enceladus-16 periapsis	Titan-119 apoapsis
Maneuver Time	23-JUN-2008 00:45:14	24-NOV-2011 05:18:00	22-MAY-2016 15:00:00
Targeting Body	Titan	Enceladus	Titan
Days to Encounter	37.8	19.6	16
Distance to Saturn	3.1 Saturn Radii	3.3 Saturn Radii	53.7 Saturn Radii
Flyby Altitude	1613.4 km	3585.8 km	975 km
True Anomaly	-45.4 deg	15.07 deg	-173.98 deg
ΔV Magnitude	12.185 m/s	2.969 m/s	0.026 m/s
Right Ascension	32.38 deg	344.82 deg	25.73 deg
Declination	64.36 deg	5.88 deg	26.88 deg
Roll Turn	88.14 deg	96.35 deg	93.4 deg
Yaw Turn	-84.74 deg	-35.89 deg	-43.22 deg
Burn Time	73.77 sec	17.17 deg	21.78 sec
Burn Type	Main Engine	Main Engine	Reaction Control System

Integration Tolerance Anomaly during the Design of OTM450

Numerical issues also arose during the design of targeting maneuvers, particularly where a very small difference in the propagator tolerance led to a significant difference in the B-Plane aimpoint parameters. As part of the routine operations process, the Cassini Orbit Determination team regularly delivered a solution which included a general inputs file (gin file) with constants and other commonly used parameters that do not change, planetary and satellite ephemerides files, and a trajectory propagated without any corrective maneuvers up to the upcoming flyby. The maneuver team then designed an OTM to ensure that the correct aimpoint parameters were achieved at the targeted flyby. As part of the regular operations procedure and before the maneuver design process was started, the maneuver team independently propagated the initial state with the gin and ephemeris files to verify that the end state matched the end state provided by the OD team. To speed things up, partials were normally not integrated. In the maneuver team propagation setup, the state tolerance

was set to 1.0×10^{-13} and the minimum step size tolerance is 1.0×10^{-9} seconds; the OD team used a state tolerance of 1.0×10^{-13} and a minimum step size tolerance of 1.0×10^{-4} seconds. This step in the design process was merely a check to ensure that the models used in the propagation by both teams are the same and the end states matched within a given tolerance.

The OD team delivered a solution on May 20, 2016 (referred to as OD1). The Cartesian initial state associated with this particular solution in EME2000 coordinates centered at Saturn Barycenter was,

$OD1_{pos} = [2741839.00069 \text{ km}, 476884.261067 \text{ km}, 1186735.49424 \text{ km}]$
$OD1_{vel} = [-1.57140839703 \text{ km/s}, 1.65990745974 \text{ km/s}, -0.545043786475 \text{ km/s}]$

and the corresponding B-Plane coordinates (B·R, B·T, time to periapsis) in EMO2000 centered at Titan were,

$OD1_{BPlane} = [3114.58870271449 \text{ km}, -2304.33548382266 \text{ km}, -7.00839062559462 \text{ sec}]$.

After receiving the OD solution, the maneuver team then routinely propagated the initial state – with the set state tolerance of 1.0×10^{-13} – and noticed a significant difference between the two end states of approximately 4.5 km in B·T and 0.56 seconds in time to periapsis, which was highly unusual. (Refer to column 1 Table 3).

Table 3. B-Plane Coordinates After Propagating the OD1 Solution to the Titan-120 Encounter

State Tolerance	1.0×10^{-13}	1.0×10^{-14}
$B \cdot R$	3114.028163354732 km	3114.588627418759 km
$B \cdot T$	-2308.878866255674 km	-2304.336068266184 km
Time To Periapsis	-7.562535022238314 sec	-7.008459605154531 sec

After trouble-shooting and changing several parameters in the propagation setup, it was found that if the state tolerance was tightened to 1.0×10^{-14}, the propagated end state matched the OD end state as expected (see column 2 Table 3). To verify that the mismatch was due to a numerical error and not due to an OD or maneuver setup error, the OD team delivered a second, very similar solution (referred to as OD2),

$OD2_{pos} = [2741839.00017 \text{ km}, 476884.26085 \text{ km}, 1186735.49498 \text{ km}]$
$OD2_{vel} = [-1.57140839602 \text{ km/s}, 1.65990745934 \text{ km/s}, -0.545043786201 \text{ km/s}]$

The corresponding B-Plane coordinates (B·R, B·T, time to periapsis) in EMO2000 centered at Titan are,

$OD2_{BPlane} = [3114.58515812081 \text{ km}, 3114.58515812081 \text{ km}, -7.00949579734326 \text{ sec}]$.

The same analysis was carried out and despite the fact that the two delivered OD solutions were almost identical, the state tolerance did not have any effect on the propagated solution. Table 4 shows the states attained with each tolerance.

Additional testing indicated that the mismatch between the end states only occurs when using a particular software version of MONTE – JPL's signature astrodynamic computing platform. For the exact same setup and other versions of MONTE, there was no discrepancy in the propagation by using the two different state tolerances. Given the proximity to the end of the mission, the Cassini

Table 4. B-Plane Coordinates After Propagating the OD2 Solution to the Titan-120 Encounter

State Tolerance	1.0×10^{-13}	1.0×10^{-14}
$B \cdot R$	3114.597763220240 km	3114.587313470157 km
$B \cdot T$	-2304.250269981904 km	-2304.333758779933 km
Time To Periapsis	-6.998480259735237 sec	-7.008626639407940 sec

Navigation Team decided that the current propagation set up would not be modified. Nonetheless, this was the first time in over 100 MONTE-designed maneuvers that the team experienced this issue. Even though the exact root cause was not determined, a tiny difference in tolerance values caused a significant difference in the B-Plane aimpoint, which from an operations standpoint, was unacceptable.

CHALLENGES FACED DURING APPROACH MANEUVER DESIGNS

A planned maneuver can be canceled if it is determined that its execution will not improve encounter conditions, yield downstream ΔV savings, or if a subsequent maneuver can attain the encounter conditions at a lower ΔV cost. There were 493 designed maneuvers from launch to end-of-mission. Even though 133 of the planned burns ended up being canceled, most of the OTMs were needed to stay close to the reference trajectory and target each flyby accurately. In certain cases, an approach maneuver was deemed necessary but too small for implementation by either propulsion system (RCS or MEA). As discussed below, OTM362 is a representative example in which the Flight Path Control Team had to redesign the burn to purposely make it large enough for implementation. In addition to dealing with too small but necessary approach maneuvers, another fairly common issue encountered during approach maneuver designs was the "near pi-transfer" singularity, in which the spacecraft flew by Titan at opposite sides of its orbit about Saturn (i.e., Titan's orbital position differed by pi radians between the two flybys).

Minimum Implementable Burn Size

A common cancelation case is an approach maneuver preceded by an accurate shaping maneuver. The cancelation criteria are subordinate to science requirements;[6] depending on science prerequisites, certain encounters admit the modification of targeting parameters. Such modification can be necessary for two reasons: (1) when a maneuver is smaller than the smallest implementable maneuver (approximately 10 mm/s), it is possible to modify the encounter time by a few tenths-of-a-second and artificially increase the maneuver magnitude and (2) some target modifications to the spatial components B·R and B·T can yield downstream ΔV savings (about 1 gram of hydrazine per mm/s saved for RCS-sized maneuvers). Both of these situations were encountered multiple times throughout the mission.

The Titan95 to Titan-96 encounter was characterized by the cancelation of the cleanup maneuver, OTM362. The decision of canceling OTM362 was made based on the fact that the designed maneuver was too small for implementation (ΔV = 7.7 mm/s). Additionally, there was virtually no downstream ΔV penalty for canceling the maneuver, i.e., the cancelation cost was -5.9 mm/s (a ΔV savings, actually). The apoapsis maneuver, OTM363, was performed, with a prohibitive downstream cost of more than 75 m/s if canceled. Finally, the approach maneuver OTM364 was

required to avoid a cancelation cost of 0.74 m/s, but the initial design of this maneuver was too small to implement. If an RCS maneuver falls under the minimum size of 10 mm/s (excluding the deadband-tightening ΔV, a plot that displays the maneuver magnitude as a function of time-of-flight (TF) bias is employed to determine the TF change necessary to raise the ΔV to the minimum level. Therefore, using 5, the amount to change the time of flight was determined. The two solutions that result in a ΔV that meets the minimum requirement are labeled. Titan-96 was modified by -0.25 seconds to increase the OTM364 ΔV magnitude to an executable size of 14.0 mm/s. Incidentally, this was the smallest RCS burn commanded at 8.2 mm/s, minus the 5.8 mm/s correction term for deadband-tightening ΔV and an observed fixed-magnitude bias ΔV in RCS burns.[7]

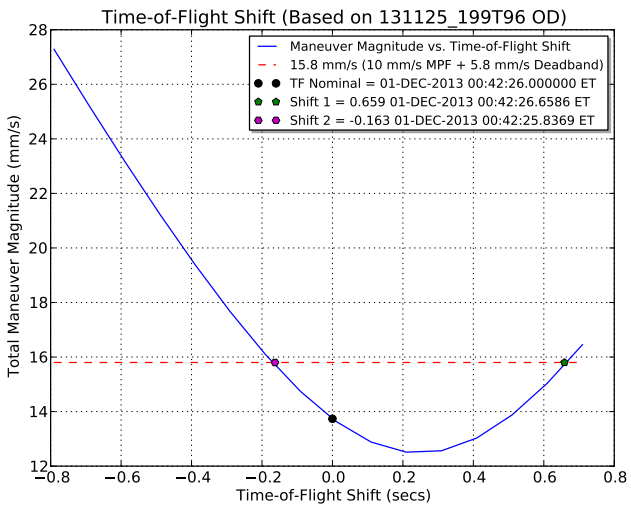

Figure 5. Titan-96 Time-of-Flight Shift via OTM364

Near Pi-Transfer Singularity

The near pi-transfer singularity was another fairly common issue encountered during approach maneuvers. A representative case is that of OTM400, the approach maneuver to the low altitude Titan-108 flyby. The Titan-107 flyby reduced the spacecraft's period to 32 days, to allow a 2:1 resonant transfer for the following two encounters. The following two maneuvers after Titan-107 were performed, with the cleanup maneuver (OTM-398) as a large RCS burn at 0.162 m/s and the apocrone maneuver (OTM-399) as a main engine burn at 0.97 m/s. The ΔV magnitude for OTM400 at the prime window was three times larger than at the backup opportunity, at 0.163 m/s versus 0.052 m/s. Additionally, the central angle (angle between the maneuver and the encounter location) for the prime window was 186.2 deg, which is near the 180 deg singularity point. At this location on the orbit, the gradients ∇(B·R), ∇(B·T), and ∇(TF) become coplanar, and the inverse of the targeting matrix used to compute the required ΔV becomes singular, making the maneuver solution extremely unstable. On the other hand, the central angle for the backup maneuver (roughly a day later) was 90.8 deg, making the solution much more stable. Therefore, only a day later and while still very close to the periapsis point, Cassini turned and fired its thrusters during the backup pass for 51 seconds providing a change in velocity of 55 mm/s to fine-tune the approach to Titan.

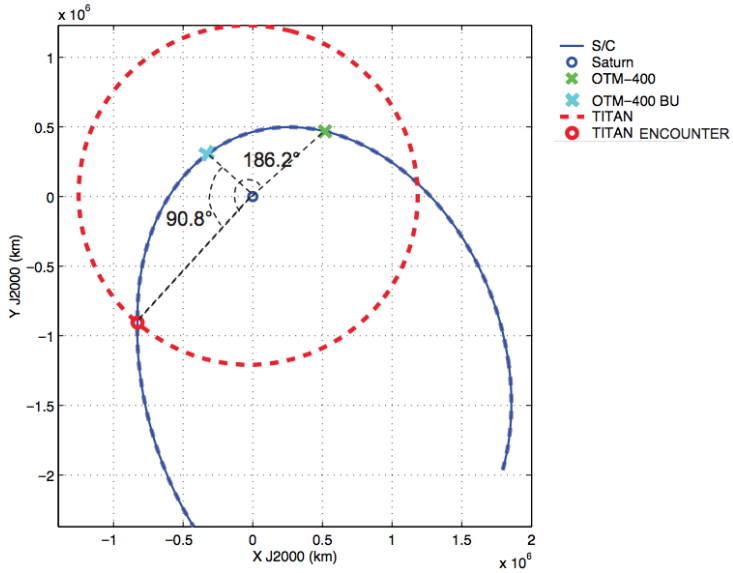

Figure 6. OTM400 maneuver locations for the Titan-108 encounter: prime and backup solutions

SINGULARITIES ENCOUNTERED DURING THE GRAND FINALE

When Cassini began its Grand Finale on April 22, 2017, navigation operations underwent a paradigm shift. Unlike the primary mission, where maneuvers were designed to precisely target the desired satellite flyby conditions, the control strategy during the Grand Finale mission was to "stay close" (within 250 km, 1σ) to the reference trajectory while minimizing the number of maneuvers and the total ΔV. To solve the problem, five years before the Grand Finale began, members of the Cassini Navigation Team examined the trades and carried out analyses used to develop the maneuver strategy for controlling the trajectory during the last phase of the Cassini mission, focusing on two tasks: 1) determining the periapse to target to along the entire reference trajectory in order to optimize the trajectory control and reduce the dispersions to a minimum and 2) once a target is selected, determining the optimal location of the targeting maneuver to minimize ΔV cost.

Minimizing ΔV using the K-Matrix

An effective and quick way of calculating the optimal maneuver location to target to the selected periapsis is to exploit certain elements of the state transition matrix (STM),[8] such that,

$$\Delta V = K^{-1}\Delta\bar{X}_f \tag{1}$$

where K is the upper right 3×3 block of the state transition matrix (ϕ), i.e.,

$$K = \begin{bmatrix} \phi_{14} & \phi_{15} & \phi_{16} \\ \phi_{24} & \phi_{25} & \phi_{26} \\ \phi_{34} & \phi_{35} & \phi_{36} \end{bmatrix} = \begin{bmatrix} \frac{\delta x_f}{\delta \dot{x}_0} & \frac{\delta x_f}{\delta \dot{y}_0} & \frac{\delta x_f}{\delta \dot{z}_0} \\ \frac{\delta y_f}{\delta \dot{x}_0} & \frac{\delta y_f}{\delta \dot{y}_0} & \frac{\delta y_f}{\delta \dot{z}_0} \\ \frac{\delta z_f}{\delta \dot{x}_0} & \frac{\delta z_f}{\delta \dot{y}_0} & \frac{\delta z_f}{\delta \dot{z}_0} \end{bmatrix} \tag{2}$$

and $\Delta\bar{X}_f$ represents the changes, or corrections, to the final state. In essence, the minimum-ΔV

location along a given rev can be calculated by evaluating the norm of the inverse of the K-matrix. That is, when $||K^{-1}||$ is minimum, then the required ΔV is also minimum. Thus, given a fixed target downstream (periapsis-j), the selected orbit for maneuver placement (from periapsis-i to periapsis-i+1) can be split into a desired number of intervals and the corresponding ΔV value can be calculated using equation 1, as illustrated in Figure 7. Once the resulting ΔV values are calculated, they are plotted as a function of time. Figure 8(a) illustrates a representative example: a maneuver is to be designed and placed between periapsis-6 and periapsis-7 with a fixed target at periapsis-12. The resulting curve figuratively represents the ΔV cost associated with placing the maneuver at any one-hour interval along the selected rev targeted to periapsis-12. The minimum point on this curve, which corresponds to the minimum ΔV location, is represented by the blue dot and the associated epoch is labeled. The specific ΔV cost in m/s is not given, but could be easily calculated using Equation 1.

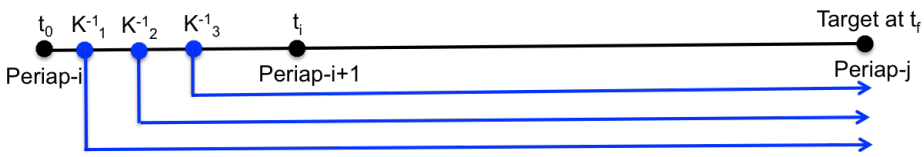

Figure 7. Schematic to illustrate how the ΔV curve is generated: blue dots indicate locations along a given rev (from periapsis-i to periapsis-i+1) at which the norm of the inverse of the K-matrix is calculated based on the state transition matrix components ($\phi_{3\times3}(t_i, t_f)$)

Two noticeable peaks appear at two different locations on the curve in Figure 8(a): one in between periapsis and apoapsis, and a second one right past apoapsis. Note that, although not clearly seen in Figure 8(a), there are spikes that form right at periapsis-6 and periapsis-7. These spikes are expected to occur and correspond to a 180-degree transfer singularity. Similarly, because of the same geometry constraint, it is expected that a peak occurs at apoapsis; however, that is not the case. There is a peak forming $near$ apoapsis. It is well-understood that there is an orbital transfer singularity due to a geometry constraint at periapsis and apoapsis (i.e., at 0, 180, and 360 degrees transfer angles). For these specific transfer angles, the Lambert problem faces a singularity. The plane of the orbit is defined by two position vectors (the space triangle). If the two position vectors are co-linear with the central mass, then the plane is undefined and a singularity in the equation arises, resulting in a ΔV of infinite magnitude (theoretically). Therefore, one would expect a peak to appear right at apoapsis when the target is placed at a periapsis downstream (180 degrees apart). In an attempt to explain why the peak is slightly shifted from the expected apse location, a two-body analysis was performed. That is, all the additional gravitational bodies initially considered in the trajectory propagation model were removed as well as the gravity harmonics for Saturn. In essence, Saturn is treated as a point mass and no other bodies are perturbing the spacecraft trajectory. If the analysis is carried out in this simplified model, then the location of the first peak shifts to apoapsis, as one would expect (refer to Figure 8(b)). Nevertheless, additional gravitational body effects and Saturn J2 terms cause the shift in the location of the first peak. Additionally, it is suspected that these extra terms have an effect on the maneuver size, i.e., they make the peaks on the ΔV curve more pronounced. Even though the second peak cannot be fully explained from an orbital geometry perspective, it can be concluded that it is not an artifact of the numerical process but rather due to a singularity in the equation caused by a transfer geometry constraint similar to the well-known 180-degree transfer problem.

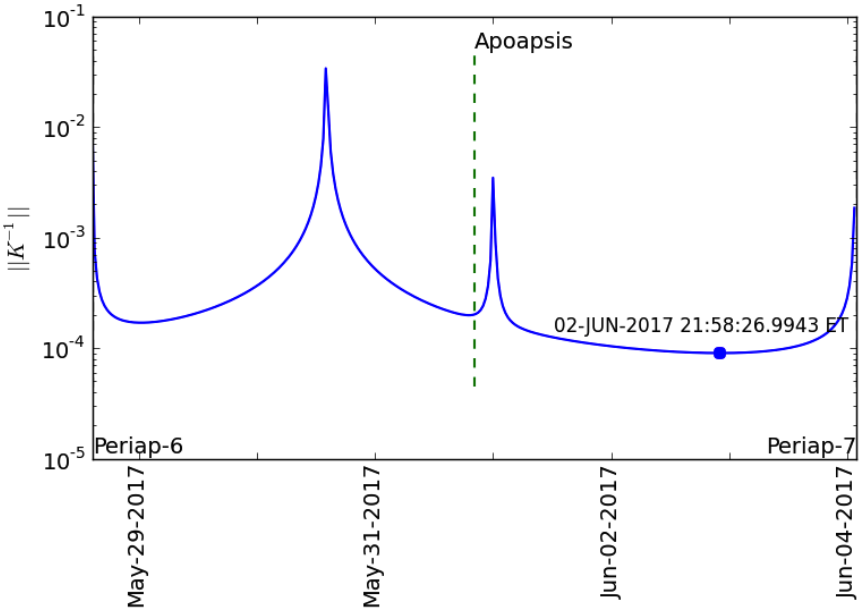

(a) Full gravitational model

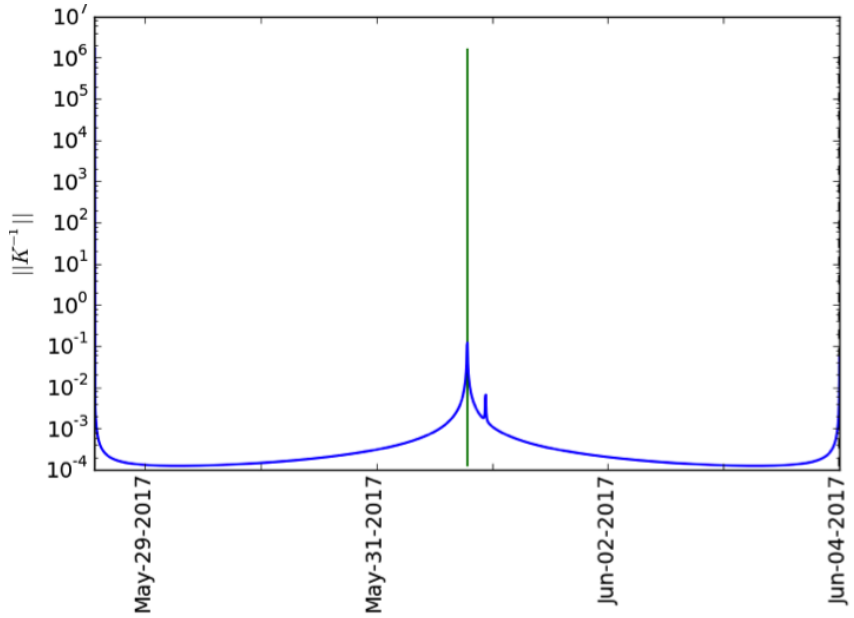

(b) Simplified gravitational model – no J2 effects

Figure 8. Norm of the inverse of the K-matrix as a function of time: minimum point on the curve represents the optimal location for maneuver placement between periapsis-6 and periapsis-7 with the target fixed at periapsis-12.

This puzzling behavior brought up several questions and multiple studies were been carried out in an attempt to explain the origin of the second peaks. In addition to studying the problem in a lower fidelity model to assess the effects of planetary harmonics and additional gravity forces, an analysis was also performed to eliminate the possibility of numerical-related issues. The potential numerical root cause was quickly ruled out by integrating individual trajectories at the given one-hour time

intervals and collecting the ΔV statistics; the cost of placing the maneuver at the peaks was indeed much higher than placing the burn elsewhere throughout the orbit. Similarly, the cost was minimum at the predicted location on the ΔV curve, which demonstrated the correlation between the linear estimate and the actual nonlinear values. Different target placement scenarios were also considered to verify that the two peaks still form even when the target is placed at a different location. That is, rather than maintaining the target always fixed at periapsis-12, every other periapsis was considered and, indeed, the peaks appeared regardless of where the target was placed. For these alternate cases, the associated ΔV values of the numerically integrated trajectories were in agreement with the linear (STM) predictions.

A gradient vector analysis was also performed to investigate any additional potential transfer geometry constraints that could explain the formation of the second peak after apoapsis only in the multi-rev targeting scenario. The three gradient vectors of interest are defined as,

$$\bar{g}_x = \begin{bmatrix} \frac{\delta x_f}{\delta \dot{x}_0} & \frac{\delta x_f}{\delta \dot{y}_0} & \frac{\delta x_f}{\delta \dot{z}_0} \end{bmatrix} \tag{3}$$

$$\bar{g}_y = \begin{bmatrix} \frac{\delta y_f}{\delta \dot{x}_0} & \frac{\delta y_f}{\delta \dot{y}_0} & \frac{\delta y_f}{\delta \dot{z}_0} \end{bmatrix} \tag{4}$$

$$\bar{g}_z = \begin{bmatrix} \frac{\delta z_f}{\delta \dot{x}_0} & \frac{\delta z_f}{\delta \dot{y}_0} & \frac{\delta z_f}{\delta \dot{z}_0} \end{bmatrix} \tag{5}$$

Two particularly useful graphs aid in this analysis: α vs. time and β vs. time. The first graph shows the time variation of α, the angle between each pair of gradient vectors (three curves) throughout the selected orbit considered for maneuver placement, i.e.,

- curve-1: angle between gradient vectors $\bar{g}_x$ and $\bar{g}_y$ (blue)
- curve-2: angle between gradient vectors $\bar{g}_y$ and $\bar{g}_z$ (green)
- curve-3: angle between gradient vectors $\bar{g}_x$ and $\bar{g}_z$ (red)

The second graph displays the time history of β, the angle between a gradient vector and its projection onto the plane formed by the other two gradient vectors (three curves), i.e.,

- curve-1: angle between gradient vector $\bar{g}_x$ and its projection onto the plane formed by gradient vectors $\bar{g}_y$ and $\bar{g}_z$ (red)
- curve-2: angle between gradient vector $\bar{g}_y$ and its projection onto the plane formed by gradient vectors $\bar{g}_x$ and $\bar{g}_z$ (green)
- curve-3: angle between gradient vector $\bar{g}_z$ and its projection onto the plane formed by gradient vectors $\bar{g}_x$ and $\bar{g}_y$ (blue)

Figure 9 shows α and β for the single-rev targeting case (maneuver placement between periapsis-6 and periapsis-7 with target fixed at periapsis-7) and Figure 10 represents α and β for the multi-rev

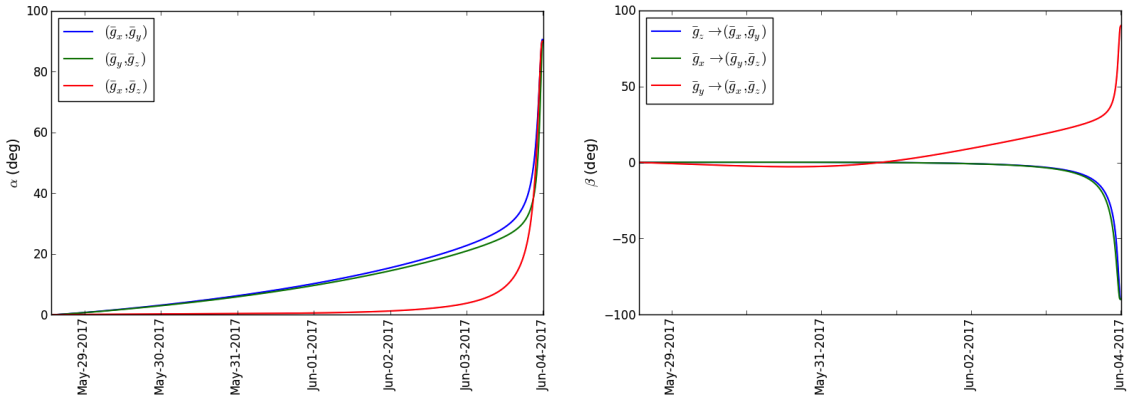

(a) α vs. Time (b) β vs. Time

Figure 9. Single-rev targeting scenario: (a) angle history between gradient vector pairs as a function of time and (b) angle evolution between gradient vector and its projection onto the plane formed by the remaining pair of gradient vectors

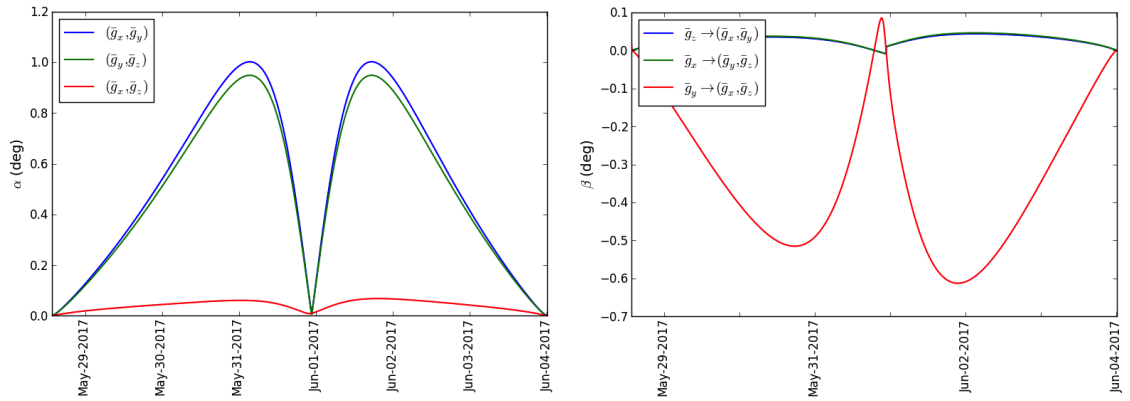

(a) α vs. Time (b) β vs. Time

Figure 10. Multi-rev targeting scenario: (a) angle history between gradient vector pairs as a function of time and (b) angle evolution between projected gradient vector onto the plane formed by the remaining pair of gradient vectors

targeting (maneuver placement between periapsis-6 and periapsis-7 with target fixed at periapsis-12). Note that the same type of behavior is exhibited in other multi-rev targeting cases, but this particular one (target at periapsis-12) is used as a representative example.

The gradient vector analysis performed for the single-rev targeting scenario reveals what is expected; when the target is fixed at the subsequent periapsis (periapsis-7), there is only one location between the selected rev (periapsis-6 to periapsis-7) where all three gradient vectors collapse onto the same plane and, hence, all three curves intersect at the origin (0 deg), corresponding to apoapsis on the orbit (180-degree transfer singularity). This result is clearly seen in in Figure 9(b). Note that, at the time of the singularity, the three gradient vectors are not collinear, as shown in Figure 9(a) (none of the three curves intersect). A more interesting situation arises when the target is fixed at more than one rev downstream (periapsis-12 in this example). Figure 10 represents the evolution of α and β with time, revealing the formation of the additional peak. That is, a second location appears

where all three gradient vectors are collinear (Figure 10(a)) and coplanar (Figure 10(b)), resulting in yet another singularity and, therefore, a much larger incurred ΔV cost.

In conclusion, the nature of the first peak is well-understood and accepted. Even though the second peak cannot be fully explained at this point from an orbital geometry perspective, it can be concluded that it is not an artifact of the numerical process but rather due to a singularity in the equation caused by a transfer geometry constraint similar to the well-known 180-degree transfer problem. It can also be concluded that additional gravitational effects such as Titan and the spherical harmonics effects of Saturn have an impact on the estimated ΔV cost.

Targeting Precisely to Periapsis

The position dispersions along the Grand Finale reference trajectory were largest at periapsis, as shown by a detailed OD covariance analysis with simulated Doppler and range tracking data.[9] As a result of this analysis, it was determined that the down-track dispersions are largest by far, with peaks at periapsis and troughs at apoapsis, indicating that the dispersions are primarily related to orbit period differences. Intuitively, one would place the target right at periapsis to control that point and minimize position dispersions with respect to the reference trajectory. However, due to the singularity in the transfer problem, targeting to periapsis precisely resulted in a drastic increase in the ΔV. As a mitigation strategy, the Cassini navigators decided to adopt the strategy of targeting just past periapsis by 2 hours, achieving practically the same control result but maintaining the propellant cost to a minimum.

REMARKS

Designing and navigating the most complex gravity-assist trajectory ever flown required continuous re-evaluation of the maneuver decision, redesign and cancellation processes. It also involved dealing with astrodynamical singularities during operations, when there was not always much time to take a step aside and evaluate the theory to understand its effects on the spacecraft path and propellant consumption. As such, the Cassini Navigation Team faced and overcame many practical, theoretical and numerical challenges. Throughout 493 maneuver designs and 160 flybys of Titan and the icy moons, the team had to deal, while in-flight, with well-known singularities in the transfer problem, numerical instabilities in state propagations through flybys, maneuver algorithm convergence issues, and orbital element targeting difficulties. As detailed in this paper, the solutions to mitigate some of these issues included moving burns to less-than-optimal locations, delaying OTMs to the backup pass to save propellant, and even increasing the size of a burn to the implementable range.

ACKNOWLEDGMENT

This research was carried out at the Jet Propulsion Laboratory, California Institute of Technology, under a contract with the National Aeronautics and Space Administration. © 2018 California Institute of Technology. Government sponsorship acknowledged.

REFERENCES

[1] B. Buffington, J. Smith, A. Petropoulos, F. Pelletier, and J. Jones, "Proposed End-Of-Mission for the Cassini Spacecraft: Inner D Ring Ballistic Saturn Impact," *61st International Astronautical Congress*, Prague, CZ, September 27-October 1 2010.

[2] D. Roth, e.a., "Cassini Tour Navigation Strategy," *AAS/AIAA Astrodynamics Specialist Conference*, Big Sky, Montana, August 3-7 2003. AAS Paper 03-546.

[3] J. Smith and B. Buffington, "Overview of the Cassini Solstice Mission Trajectory," *AAS/AIAA Astrodynamics Specialist Conference*, Pittsburgh, Pennsylvania, August 9-13 2009. AAS Paper 09-351.

[4] B. Buffington, N. Strange, and J. Smith, "Overview of the Cassini Extended Mission Trajectory," *AAS/AIAA Astrodynamics Specialist Conference*, Honolulu, Hawaii, August 18-21 2008. AIAA-2008-6752.

[5] P. W. Stumpf, E. M. Gist, T. D. Goodson, Y. Hahn, S. V. Wagner, and P. N. Williams, "Flyby Error Analysis Based on Contour Plots for the Cassini Tour," *Journal of Spacecraft and Rockets*, Vol. 46, 2009, p. 5.

[6] P. N. Williams, E. M. Gist, T. D. Goodson, Y. Hahn, P. W. Stumpf, and S. V. Wagner, "Orbit Control Operations for the Cassini-Huygens Mission," *SpaceOps 2008 Conference,* AIAA-2008-3429, Heidelberg, Germany, May 12–16, 2008.

[7] M. Vaquero, Y. Hahn, P. Stumpf, P. N. Valerino, S. V. Wagner, and M. Wong, "Cassini Maneuver Experience for the Fourth Year of the Solstice Mission," *AIAA/AAS Astrodynamics Specialist Conference*, San Diego, California, August 4-7 2014. AIAA Paper 2014-4348.

[8] M. Vaquero, Y. Hahn, D. Roth, and M. Wong, "A Linear Analysis for the Flight Path Control of the Cassini Grand Finale Orbits," *26th International Symposium on Space Flight Dynamics*, Matsuyama, Japan, June 3-9 2017. AAS Paper 03-546.

[9] M. Wong, Y. Hahn, D. Roth, and M. Vaquero, "Trajectory Dispersion Control for the Cassini Grand Finale," *25th International Symposium on Space Flight Dynamics*, Munich, Germany., October 19-23 2016.